Electronic Supplementary Material (ESI) for CrystEngComm.
This journal is © The Royal Society of Chemistry 2018

Electronic Supplementary Information

Capturing a new hydrate polymorph of amodiaquine dihydrochloride dihydrate via heterogeneous crystallisation

Okky Dwichandra Putra[a,d], Anna Pettersen[b], Sten O. Nilsson-Lill[b], Daiki Umeda[c], Etsuo Yonemochi[c], Yuda Prasetya Nugraha[d], Hidehiro Uekusa[d*]*

[a]Pharmaceutical Development and [b]Early Product Development, Pharmaceutical Sciences, AstraZeneca Gothenburg, Pepparedsleden 1, Mölndal SE-431 83, Sweden

[c]School of Pharmacy and Pharmaceutical Sciences, Hoshi University, 2-4-41, Ebara, Shinagawa, Tokyo 142-8501, Japan

[d]Department of Chemistry, Tokyo Institute of Technology, Ookayama 2-12-1, Meguro-ku, Tokyo, 152-8551

E-mail: okky.putra@astrazeneca.com (O.D.P.); uekusa@chem.titech.ac.jp (H.U.)

Materials and Methods

1. Materials

Known form of amodiaquine dihydrochloride dihydrate (Batch no. AMH–113003) and magnesium chloride hexahydrate were purchased from Mangalam Drugs & Organics Ltd. (Mumbai, India) and Naqalai Tesque (Tokyo, Japan), respectively. These compounds were used as received for all processes. Other chemicals used in this study were purchased from Nacalai Tesque (Tokyo, Japan) and used without further purification.

2. Methods

2.1 Crystallization experiment

An equimolar mixture consisting known form of amodiaquine dihydrochloride dihydrate (46.4 mg, 0.1 mmol) and magnesium chloride hexahydrate (20.3 mg, 0.1 mmol) was dissolved in 50 mL methanol. The resulting solutions were incubated at ambient temperature for 2 weeks, yielding yellow needle-shaped crystals suitable for single-crystal X-ray diffraction.

2.2 Powder X-ray diffraction (PXRD)

PXRD measurements were performed using a SMART-LAB X-ray diffractometer (Rigaku, Japan). The corresponding patterns were collected in reflection mode for $2\theta = 3–40°$ at 25 °C with a step of 0.01° and a scan speed of 20° min^{-1} (Cu Kα source, 45 kV, 200 mA).

2.3 Single crystal diffraction and refinements

Single-crystal X-ray diffraction data were collected at 93(2) K in the ω-scan mode with an R-AXIS RAPID II (Rigaku, Japan) using Cu–Kα X-rays obtained from a rotating anode source with focused mirror optics ($\lambda = 1.541865$ Å). The integrated and scaled data were empirically corrected for absorption effects using ABSCOR,[1] and the initial structure was solved with SIR 2014[2] using the direct method and refined on F_0^2 with SHELXL 2014.[3] All non-hydrogen atoms were anisotropically refined, and hydrogen atom positions were calculated geometrically and included in the calculation using the riding model. Hydrogen atoms attached to oxygen and nitrogen atoms were located using a differential

Fourier map. All hydrogen atoms were freely refined, and molecular graphics were produced using Mercury 3.10 software.

2.4 Differential thermal analysis (DTA) and thermogravimetric (TG)

DTA and TG measurements were performed using a TG-DTA 9320 (Rigaku, Japan). Approximately 15 mg of samples TG were accurately weighed into aluminum pans. The sample pans were heated at a rate of 3 °C min^{-1} from 25 to 150 °C and an empty aluminum pan was used as reference. Open pan was used for DTA-TG measurements.

2.5 Dynamic vapour sorption (DVS)

Vapor sorption isotherms were measured by DVS at 25 °C using a Dynamic Vapor Sorption Advantage instrument (SMS Ltd., London, UK). Sieved samples were mounted on a balance and relative humidity (RH) was increased from 0 to 80% with 5% steps. The waiting time for 0.001% weight change was set to 15 min and the further step was increased or decreased automatically.

2.5 Dispersion corrected density functional theory (DFT-D) calculations

Density functional theory calculations were carried out by using CASTEP in Materials Studio 7.0 package. The GGA-PBE functional was used with quality settings set to fine. Cut-off energy was set to 520 eV and a k-point separation of 0.05 Å-1 was used. Grimme's D2 dispersion correction was employed.

3. Results

Table S1 List of other salt used in heterogenous crystallization

NaCl
KCl
LiCl
$MgCl_2$. $6H_2O$
$CaCl_2$
$FeCl_3$ and $FeCl_3.6H_2O$
$CoCl_2$
$NiCl_2$. $6H_2O$
$CuCl_2$. $2H_2O$

Table S2 Crystallographic details of new AQ polymorph

Chemical formula	$C_{20}H_{24}ClN_3O\cdot2(Cl)\cdot2(H_2O)$
M_r	464.80
Crystal system, space group	Monoclinic, $P2_1/n$
Temperature (K)	173
a, b, c (Å)	7.69610(14), 10.9153(2), 27.2368(5)
β (°)	96.1341(7)
V (Å^3)	2274.93 (7)
Z	4
Radiation type	Cu $K\alpha$
μ (mm^{-1})	3.86
Crystal size (mm^3)	0.41 × 0.09 × 0.05
Diffractometer	Rigaku RAPID AXIS-II SPIDER
T_{min}, T_{max}	0.123, 0.987
No. of measured, independent and observed [$I > 2\sigma(I)$] reflections	19441, 3083, 2665
R_{int}	0.062
$(\sin \theta/\lambda)_{max}$ (Å^{-1})	0.062
$R[F^2 > 2\sigma(F^2)]$, $wR(F^2)$, S	0.044, 0.114, 1.09
No. of reflections	3083
No. of parameters	296
$\Delta\rho_{max}$, $\Delta\rho_{min}$ (e Å^{-3})	0.56, −0.22

Table S3 Hydrogen bond parameters (distance, in Å and angle, in degrees) determined for AQ

	New form					Previously known form[4]				
Interaction	D−H	H···A	D···A	D−H···A	Symmetry Operation	D−H	H···A	D···A	D−H···A	Symmetry Operation
N1−H···Cl2	0.95(3)	2.24(3)	3.170(2)	167(3)	-*x*+1,-*y*-1,-*z*+1	0.89(2)	2.32(2)	3.1913(16)	166.8(19)	
N2−H···O3	0.87(3)	2.04(3)	2.887(3)	162(2)		0.83(2)	2.07(2)	2.880(2)	167(2)	*x*,1/2-*y*,-1/2+*z*
N3−H···Cl3	0.94(3)	2.16(3)	3.063(2)	160(2)		0.85(2)	2.26(2)	3.0771(14)	161(2)	
O1−H···Cl2	0.76(3)	2.29(3)	3.046(2)	170(3)	-*x*+3/2,*y*+1/2,-*z*+3/2	0.84	2.22	3.0640(12)	177	-1-*x*,-1/2+*y*,1/2-*z*
O2−H···Cl3	0.851(18)	2.38(2)	3.189(3)	160(4)		0.88(3)	2.30(3)	3.1778(16)	175(3)	-*x*,-1/2+*y*,1/2-*z*
O2−H···Cl3	0.868(18)	2.34(2)	3.208(2)	173(3)	-*x*+2,-*y*-1,-*z*+1	0.80(3)	2.42(3)	3.2100(16)	171(3)	*x*,1/2-*y*,-1/2+*z*
O3−H···O2	0.851(18)	1.934(19)	2.782(3)	174(4)	-*x*+2,-*y*,-*z*+1	0.83(3)	1.95(3)	2.775(2)	174(2)	
O3−H···Cl2	0.832(17)	2.360(18)	3.178(2)	168(3)	*x*,*y*+1,*z*	0.83(3)	2.33(3)	3.1585(15)	173(3)	-1-*x*,-1/2+*y*,1/2-*z*

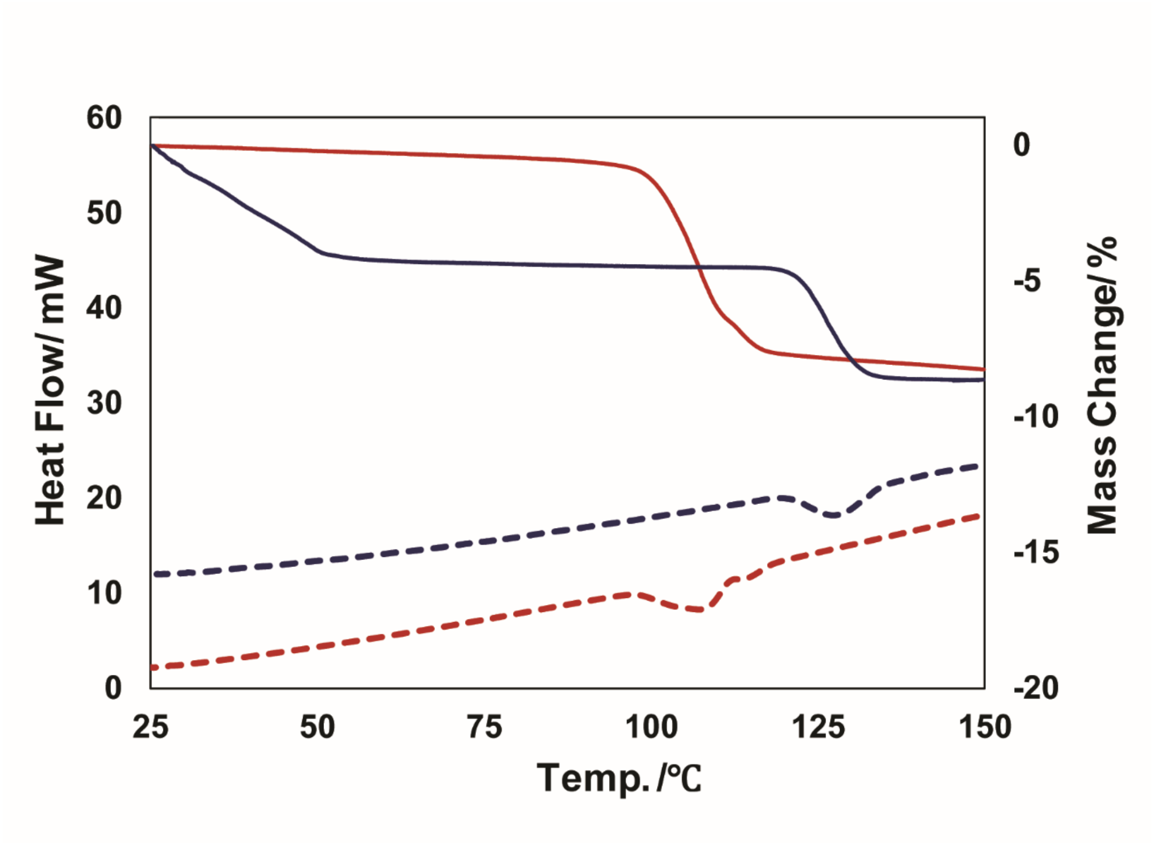

Figure S1 TG and DTA scans of new (blue) and known (red) of AQ. Solid and dashed lines represents TG and DTA scans, respectively.

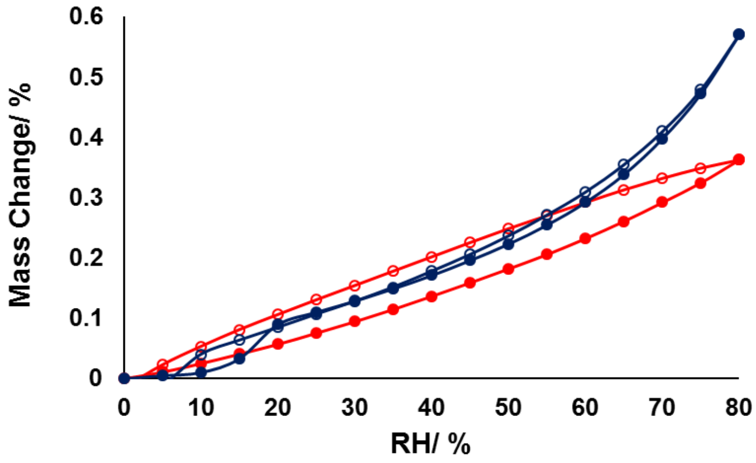

Figure S2 Water sorption–desorption of new (blue) and known (red) of AQ. The closed and open symbols represent sorption and desorption, respectively.

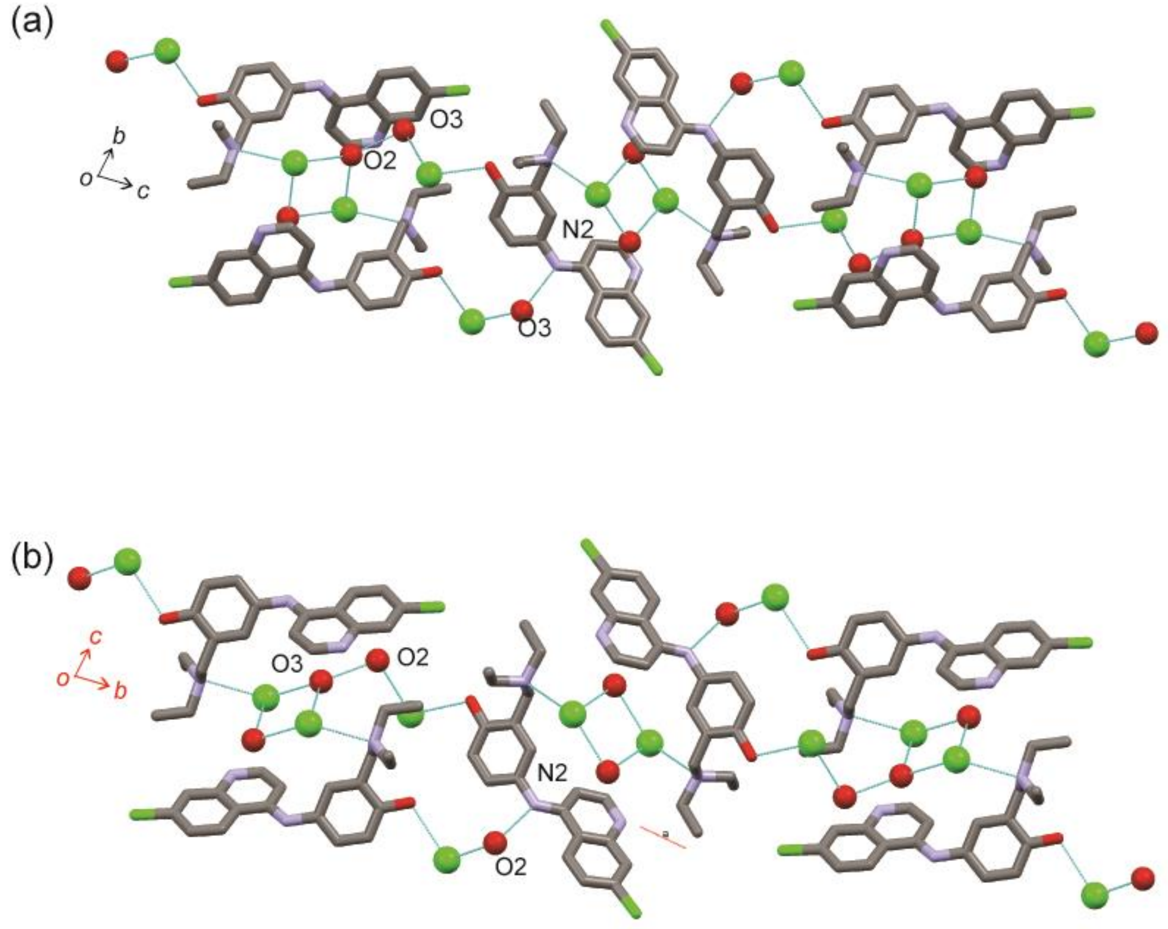

Figure S3 One dimensional (1D) chain structure in (a) new and (b) known polymorphs of AQ.

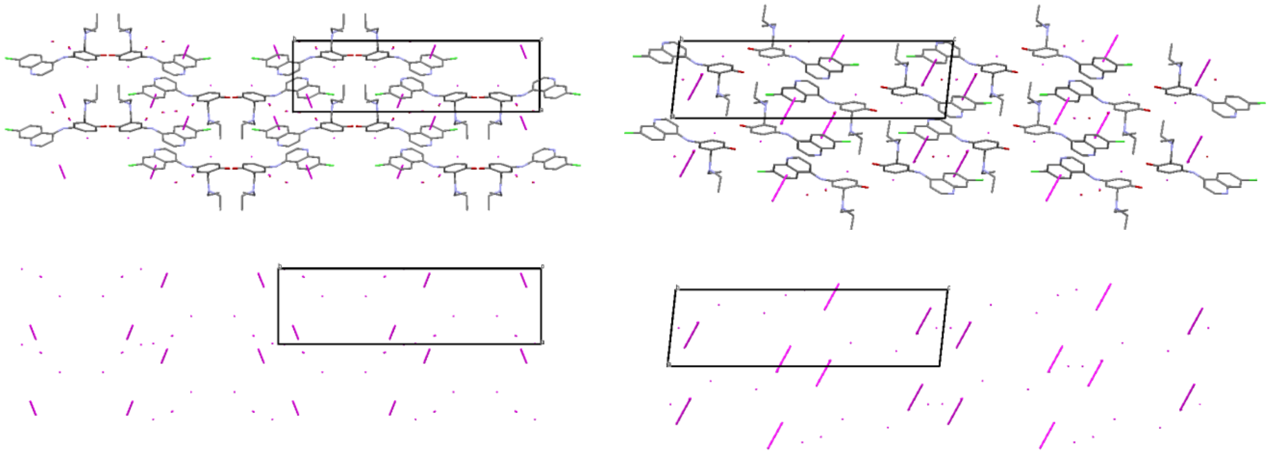

Figure S4. Visualization of strongest interaction, represented as blue lines, calculated using B3LYP/6-31G(d,p) for previously known (left) and new polymorph (right) of AQ.

Reference

1. Calculated using ABSCOR: Empirical Absorption Correction Based on Fourier Series Approximation; Rigaku: The Woodlands, TX, 1994.
2. Burla, M. C.; Caliandro, R.; Camalli, M.; Carrozzini, B.; Cascarano, G. L.; De Caro, L.; Giacovazzo, C.; Polidori, G.; Spagna, R. *J. Appl. Crystallogr*. 2005, **38**, 381–388.
3. Sheldrick, G. M. *Acta Crystallogr., Sect. A: Found. Crystallogr*. 2008, **64**, 112– 122.
4. Kimpende, P. M.; van Meervelt, L. *Acta Crystallogr., Sect. E: Struct. Rep. Online*, 2010, **66**, o2353-o2354.